

An Extreme Amplitude, Massive Heartbeat System in the LMC Characterized Using ASAS-SN and TESS

T. Jayasinghe^{1,2*}, K. Z. Stanek^{1,2}, C. S. Kochanek^{1,2}, Todd A. Thompson^{1,2,3},
B. J. Shappee⁴, M. Fausnaugh⁵

¹Department of Astronomy, The Ohio State University, 140 West 18th Avenue, Columbus, OH 43210, USA

²Center for Cosmology and Astroparticle Physics, The Ohio State University, 191 W. Woodruff Avenue, Columbus, OH 43210, USA

³Institute for Advanced Study, Princeton, NJ, 08540, USA

⁴Institute for Astronomy, University of Hawaii, 2680 Woodlawn Drive, Honolulu, HI 96822, USA

⁵MIT Kavli Institute for Astrophysics and Space Research, 77 Massachusetts Avenue, 37-241, Cambridge, MA 02139, USA

Accepted XXX. Received YYY; in original form ZZZ

ABSTRACT

Using ASAS-SN data, we find that the bright ($V \sim 13.5$ mag) variable star MACHO 80.7443.1718 (ASASSN-V J052624.38-684705.6) is the most extreme heartbeat star yet discovered. This massive binary, consisting of at least one early B-type star, has an orbital period of $P_{\text{ASAS-SN}} = 32.83627 \pm 0.00846$ d, and is located towards the LH58 OB complex in the LMC. Both the ASAS-SN and TESS light curves show extreme brightness variations of $\sim 40\%$ at periastron and variations of $\sim 10\%$ due to tidally excited oscillations outside periastron. We fit an analytical model of the variability caused by the tidal distortions at pericenter to find orbital parameters of $\omega = -61.4^\circ$, $i = 44.8^\circ$ and $e = 0.566$. We also present a frequency analysis to identify the pulsation frequencies corresponding to the tidally excited oscillations.

Key words: stars: early-type – stars: oscillations – stars: massive – stars: variables: general – (stars:) binaries: general

1 INTRODUCTION

Heartbeat stars are short period ($P \lesssim 1$ yr), eccentric ($e \gtrsim 0.3$) binaries where oscillations are excited by the tidal forcing at each periastron passage. Heartbeat stars were first discovered in data from the *Kepler* space telescope (Thompson et al. 2012). The prototypical heartbeat star, KOI-54, has been extensively studied and characterized (see for e.g., Welsh et al. 2011; Fuller, & Lai 2012; Burkart et al. 2012 and references therein), and *Kepler* (Kirk et al. 2016) has now identified over 170 heartbeat stars.

The light curves of heartbeat stars are defined by oscillations outside of periastron combined with a brief, high amplitude ellipsoidal variation at periastron that gives rise to a unique “heartbeat” signature resembling the normal sinus rhythm of an electrocardiogram. The light curves of these systems are dominated by the effects of tidal distortion, reflection and Doppler beaming close to periastron (Fuller 2017). Heartbeat stars continue to oscillate throughout their orbit due to tidally excited stellar oscillations. The variability amplitude of most heartbeat stars is very small ($\lesssim 1$ mmag; Kirk et al. 2016; Hambleton et al. 2018).

The tidally excited oscillations (TEOs) occur at exact integer

multiples of the orbital frequency (Fuller 2017). TEOs were first discovered in the eccentric binary system HD 174884 (Maceroni et al. 2009) and later confirmed in KOI 54 and several other systems (Shporer et al. 2016). The largest amplitude TEOs are driven by resonances between harmonics of the orbital frequency and the normal mode frequencies of the star. Both the amplitudes and phases of TEOs can be predicted from linear theory (Fuller 2017).

The vast majority of the heartbeat stars that have been discovered are relatively low-mass A and F type stars. However, the heartbeat phenomenon extends to more massive OB stars as well. ι Ori is the most massive heartbeat star system yet discovered and it consists of a O9 III primary and a B1 III-IV companion (Pablo et al. 2017). The dearth of massive heartbeat stars is likely an observational bias because massive stars are rare and *Kepler* observed only a small fraction of the sky, mostly lying off the Galactic plane. Ground-based surveys cover most or all of the sky but find it challenging to detect the low variability amplitudes of typical heartbeat stars ($\Delta L/L \sim 10^{-3}$; Fuller 2017).

The All-Sky Automated Survey for SuperNovae (ASAS-SN, Shappee et al. 2014; Kochanek et al. 2017) has been monitoring the entire visible sky for several years to a depth of $V \lesssim 17$ mag with a cadence of 2–3 days using two units in Chile and Hawaii, each with 4 telescopes. As of the end of 2018, ASAS-SN uses 20 telescopes to

* E-mail: jayasinghearachilage.1@osu.edu

observe the entire sky daily, but all current observations are taken with a *g*-band filter. We have written a series of papers studying variable stars using ASAS-SN data. In Paper I (Jayasinghe et al. 2018a), we reported ~66,000 new variables that were discovered during the search for supernovae. In Paper II (Jayasinghe et al. 2019a), we homogeneously analyzed ~412,000 known variables from the VSX catalog, and developed a robust variability classifier utilizing the ASAS-SN V-band light curves and data from external catalogues. In Paper III (Jayasinghe et al. 2019b), we conducted a variability search towards the Southern Ecliptic pole in order to overlap with the The Transiting Exoplanet Survey Satellite (TESS; Ricker et al. 2015) continuous viewing zone (CVZ). We identified ~11,700 variables, of which ~7,000 were new discoveries.

TESS is currently conducting science operations by monitoring (eventually) most of the sky with a baseline of at least 27 days. Sources closer to the TESS CVZ will be observed for a substantially longer period, approaching one year at the ecliptic poles. TESS full-frame images (FFIs), sampled at a cadence of 30 min, are made publicly available, allowing for the study of short time scale variability across most of the sky.

Here we discuss the identification of the most extreme amplitude heartbeat star yet discovered, MACHO 80.7443.1718 (ASASSN-V J052624.38-684705.6, TIC 373840312), using both ASAS-SN and TESS photometry. The MACHO survey reported that the source was a variable, but classified it as an eclipsing binary (Alcock et al. 1997). MACHO 80.7443.1718 was first identified as a likely heartbeat star during our ASAS-SN variability search. We discuss archival data and the ASAS-SN and TESS observations in section 2. In section 3, we fit an analytical model for the tidal distortions to estimate several orbital parameters of the binary system. In section 4, we discuss our SED fits to this source and the physical implications of these fits. In section 5, we identify tidally excited oscillations through a periodogram analysis and present a summary of our results in section 6.

2 ARCHIVAL, ASAS-SN AND TESS DATA FOR MACHO 80.7443.1718

The source MACHO 80.7443.1718 was identified as a variable by the MACHO survey (Alcock et al. 1997), who classified it as a generic eclipsing binary. Two values for the orbital period, corresponding to the “red” and “blue” bandpasses, were derived using their data: $P_{\text{red}} = 32.83108$ d, $P_{\text{blue}} = 32.83397$ d.

MACHO 80.7443.1718 is a blue source with $U - B = -0.84$ mag, $B - V = 0.11$ mag with estimated values for the photometric temperature $\log(T_*/\text{K}) = 4.6$ and bolometric magnitude $M_{\text{bol}} = -9.1$ (Massey 2002). This source is part of the LH58 OB association in the Large Magellanic Cloud (LMC), northwest of 30 Doradus. An archival spectrum classified it as a B0.5 Ib/II (Garmany et al. 1994), evolved blue star. Based on this information, this source is likely to have a mass $M \gtrsim 10M_{\odot}$ (Nieva & Przybilla 2014).

The Gaia DR2 (Gaia Collaboration et al. 2018) counterpart is source_id=4658489067332871552. Its nominal DR2 parallax is negative ($\pi = -0.0586 \pm 0.0238$ mas) and the proper motion is $\mu_{\alpha} = 1.59 \pm 0.04$ mas yr⁻¹, $\mu_{\delta} = 0.66 \pm 0.05$ mas yr⁻¹. There might be evidence of problems with the astrometric solution, as the χ^2 of the fit is high and the excess astrometric noise is 0.14 mas. On the other hand, the renormalized unit weight error (RUWE; Lindegren et al. 2018) of the source is 0.96 and Lindegren et al. (2018) argue that Gaia DR2 astrometric solutions are accurate if they have a RUWE < 1.4.

To evaluate the proper motions, we examined 56 Gaia DR2 stars with $G < 15$ mag within 5' of MACHO 88.7443.1718. These 56 stars had medians (1σ range) of -0.024 mas ($-0.126 < \pi < 0.020$), 1.670 mas yr⁻¹ ($0.540 < \mu_{\alpha} < 1.814$) and 0.697 mas yr⁻¹ ($0.125 < \mu_{\delta} < 0.852$) for their parallax and proper motions. Hence the parallax and proper motions of MACHO 88.7443.1718 are typical of the local population of luminous stars. If we use the median proper motions to define a local standard of rest, the relative motion of MACHO 88.7443.1718 is 0.088 mas yr⁻¹, or roughly 21 km s⁻¹ at a distance of 50 kpc. The median motion of the nearby stars relative to this standard of rest is 0.215 mas yr⁻¹ or roughly 50 km s⁻¹.

ASAS-SN V-band observations were made by the “Cassius” (CTIO, Chile) quadruple telescope between 2013 and 2018. Each camera has a field of view of 4.5 deg², the pixel scale is $8''/0$ and the FWHM is ~2 pixels. The light curves for this source was extracted as described in Kochanek et al. (2017) using aperture photometry with a 2 pixel radius aperture. The AAVSO Photometric All-Sky Survey (APASS; Henden et al. 2015) DR9 catalog was used for absolute photometric calibration. The ASAS-SN V-band light curve has a time baseline of ~1669 d. We derived possible periods for this source following the procedure described in Jayasinghe et al. (2018a, 2019a). The *astrobase* implementation (Bhatti et al. 2018) of the Generalized Lomb-Scargle (GLS, Zechmeister & Kürster 2009; Scargle 1982), the Multi-Harmonic Analysis Of Variance (MHAOV, Schwarzenberg-Czerny 1996), and the Box Least Squares (BLS, Kovács et al. 2002) periodograms were used to search for periodicity in these light curves. We calculated the Lafler-Kinmann (Lafler & Kinman 1965; Clarke 2002) string length statistic $T(\phi|P)$ on the phased light curve for each period using the definition

$$T(\phi|P) = \frac{\sum_{i=1}^N (m_{i+1} - m_i)^2}{\sum_{i=1}^N (m_i - \bar{m})^2} \times \frac{(N-1)}{2N} \quad (1)$$

from Clarke (2002), where the m_i are the magnitudes sorted by phase and \bar{m} is the mean magnitude. The best period is the period with the smallest $T(\phi|P)$, which in this case is the best BLS period.

$$P_{\text{ASAS-SN}} = 32.83627 \pm 0.00846 \text{ d,}$$

which agrees with the MACHO periods to within ~0.02%. The ASAS-SN light curve hence contains ~50 orbits of this system. The error in the period was estimated using the spacing in the BLS frequency grid ($\Delta f = 7.84 \times 10^{-6}$ day⁻¹), where $\Delta P = \Delta f / f^2 = 0.00846$ d.

MACHO 80.7443.1718 lies in the Southern TESS CVZ which allowed us to extract TESS light curves for both Sectors 1 and 2. Due to the large pixel size of TESS (21") and the crowded region surrounding MACHO 80.7443.171, we used image subtraction (Alard & Lupton 1998; Alard 2000) on the full frame images (FFIs) from the first TESS data release to produce high fidelity light curves. The 27 day baseline for TESS observations in each sector is insufficient to obtain a full orbit for this source, but the final TESS light curve with data from all the sectors in the south should sample the variability of this source very well. The difference light curve was normalized to match the ASAS-SN V-band light curve.

The ephemeris for the minimum of the ellipsoidal variation in ASAS-SN is

$$\text{EphemI} = \text{BJD } 2458143.698310 + 32.83627 \times E, \quad (2)$$

whereas the ephemeris for the minimum of the ellipsoidal variation in TESS is

$$\text{EphemII} = \text{BJD } 2458373.61518 + 32.83627 \times E, \quad (3)$$

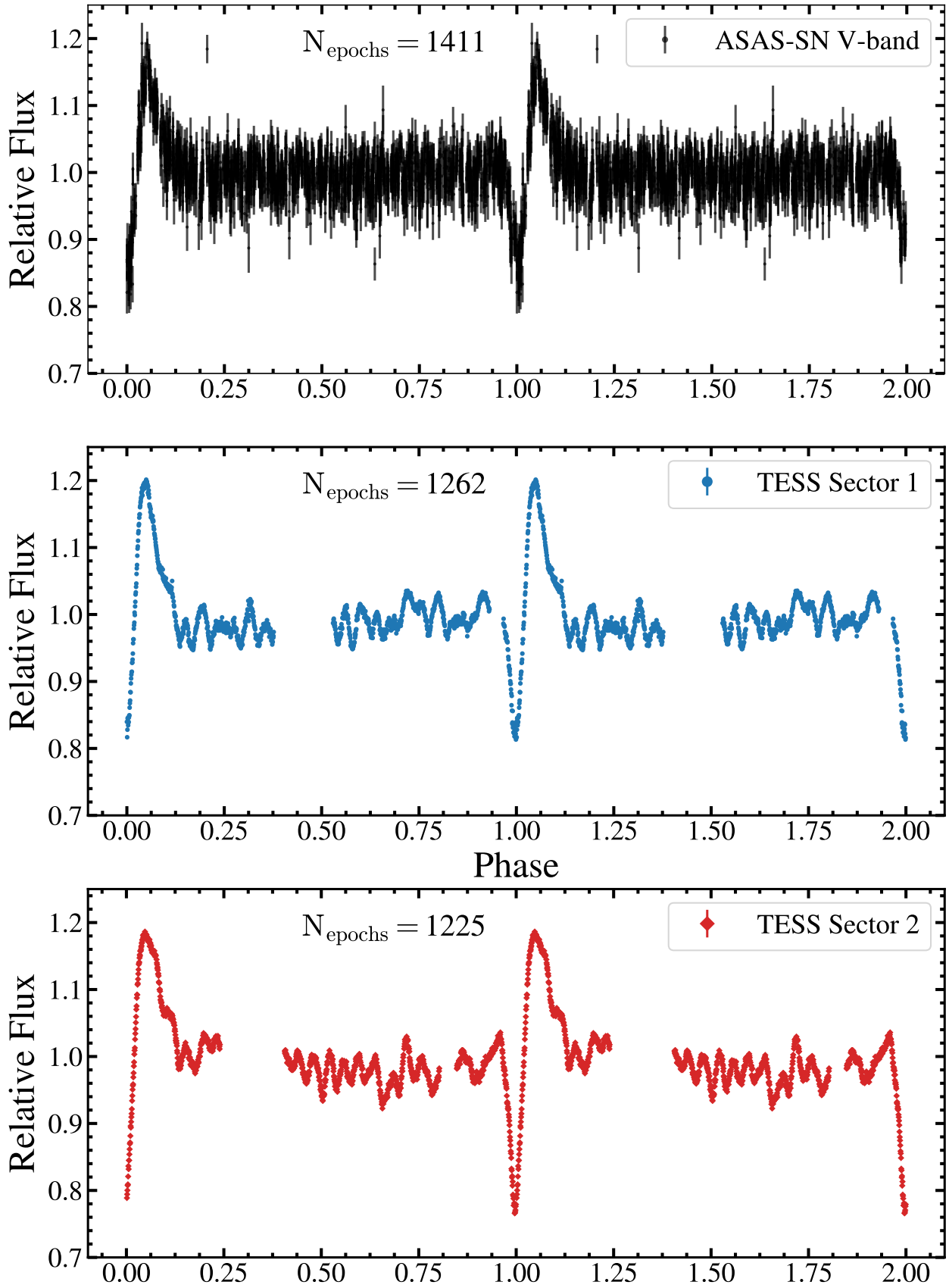


Figure 1. The phased ASAS-SN (top), TESS sector 1 (middle), and TESS Sector 2 (bottom) light curves for the source MACHO 80.7443.1718.

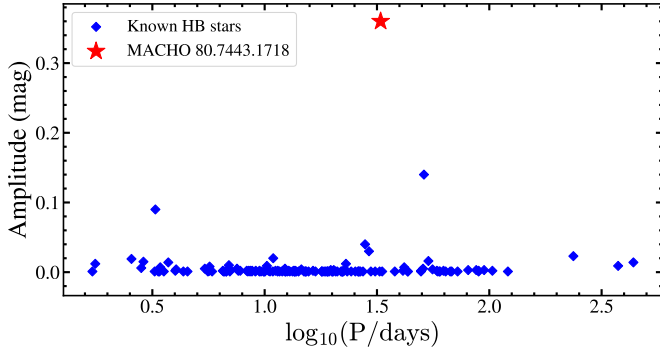


Figure 2. The period-amplitude diagram for the sample of heartbeat stars. Heartbeat stars listed in the VSX database (Watson et al. 2006) are indicated by blue diamonds. MACHO 80.7443.1718 (this work) is shown with a red star.

where the epoch E is the number of orbits since the time of minimum.

The phased ASAS-SN and TESS Sector 1+2 light curves are shown in Figure 1. The uncertainties in relative flux are virtually indistinguishable from the points in the TESS light curves. The TEOs are clearly visible in the TESS light curves (red and green points), but are less distinguishable in the ASAS-SN light curve (blue points).

The peak-to-peak flux variations at periastron of $\sim 40\%$ (~ 0.36 mag) are the largest observed for a heartbeat system. This is illustrated in Figure 2, where we compare the period and amplitude of MACHO 80.7443.1718 to those of the heartbeat stars in the VSX catalog (Watson et al. 2006). The flux variations outside of periastron are also extreme (~ 0.1 mag). Fuller (2017) notes that very large amplitude TEOs are unlikely to arise from a chance resonance and are more likely to stem from a resonantly locked mode.

3 MODELLING THE ECCENTRIC ELLIPSOIDAL VARIATIONS

Kumar et al. (1995) developed an analytical model (their Equation 44) for the flux variations produced by the tidal distortions produced by eccentric binaries at periastron. Thompson et al. (2012) successfully applied this model to fit the light curves of the heartbeat stars observed by *Kepler*. We fit the fractional flux $\delta F/F$ of the ASAS-SN and TESS light curves following Thompson et al. (2012). The fit contains six parameters: the amplitude scaling factor, S , a fractional flux offset, C , the true anomaly, $\phi(t)$, the angle of periastron, ω , the orbital inclination, i and the eccentricity, e ,

$$\frac{\delta F}{F} = S \frac{1 - 3 \sin^2(i) \sin^2(\phi(t) - \omega)}{(R(t)/a)^3} + C, \quad (4)$$

where

$$\frac{R(t)}{a} = 1 - e \cos(E), \quad (5)$$

$$\phi(t) = 2 \arctan \left(\sqrt{\frac{1+e}{1-e}} \tan \left(\frac{E}{2} \right) \right), \quad (6)$$

and the eccentric anomaly (E) is derived from solving Kepler's

Table 1. Best fit parameters for MACHO 80.7443.1718

Description		ASAS-SN	TESS
ω	Angle of periastron	$-54.50^\circ \pm 1.15^\circ$	$-61.35^\circ \pm 0.02^\circ$
i	Orbital inclination	$48.01^\circ \pm 0.42^\circ$	$44.77^\circ \pm 0.01^\circ$
e	Orbital Eccentricity	0.566 ± 0.004	0.565 ± 0.002

transcendental equation (e.g., Murray & Correia 2010). We performed a trial fit through the Levenberg-Marquardt chi-square minimization routine in `scikit-learn` (Pedregosa et al. 2012). The parameters from the trial fit were then used to initialize a Monte Carlo Markov Chain sampler (MCMC) with 100 walkers, and was then run for 5000 iterations. We used the MCMC implementation through `emcee` (Foreman-Mackey et al. 2013). The errors in the parameters were derived from the MCMC chains.

These fits do not capture the depth of the minimum or the height of the maximum completely, suggesting that this model is an incomplete description of the light curve. Formally, the estimates for ω and i from fitting the ASAS-SN and TESS light curves differ by 3σ , but the actual differences of $< 7^\circ$ are remarkably small given the very different characters of the two light curves. The eccentricities derived from the two fits are consistent to within 1σ . While this model does not account for effects such as irradiation and Doppler boosting, it is a good approximation of the tidal distortions during the orbit and can be used to estimate the orbital parameters of this system without requiring further knowledge about the properties of the stars in the system. The best-fit models for the ASAS-SN and combined Sector 1+2 TESS data for MACHO 80.7443.1718 are shown in the top panel of Figure 3 with the solid red lines. The best fit parameters are summarized in Table 1.

We attempted fitting a standard eclipsing binary model including irradiation and reflection effects to the ASAS-SN V-band light curve using PHOEBE 2.1 (Prša et al. 2016; Horvat et al. 2018) but were unable to replicate the observed variability amplitude. This is not very surprising because the high amplitude pulses are almost certainly due to transient dynamical tides that are not included in normal eclipsing binary modeling codes. Unfortunately, there are no public codes for modeling heartbeat stars which include these effects. We have put off attempts at more detailed models until we have the radial velocity data needed to better constrain the orbit and masses. We will also explore a simultaneous fit to the light curve incorporating both the binary star features and the tidally induced pulsations with PHOEBE 2.1 (see for e.g., Hambleton et al. 2018).

4 SED FITTING

We fit the spectral energy distribution (SED) of MACHO 80.7443.1718 using the 15 photometric measurements spanning $3.6\mu\text{m}$ through U band given in Table 2 using DUSTY (Ivezic & Elitzur 1997; Elitzur & Ivezic 2001) inside a Markov Chain Monte Carlo wrapper (Adams & Kochanek 2015). We assumed foreground extinction due to $R_V = 3.1$ dust (Cardelli et al. 1989) and used Castelli & Kurucz (2004) model atmospheres for the star. We assume the source is in the LMC at a distance of $d_{\text{LMC}} = 50$ kpc (Pietrzyński et al. 2013). Even when assuming minimum luminosity uncertainties of 10% for each band, the fits have $\chi^2/N_{\text{dof}} \approx 6$ at fixed T_* . While this is adequate for determining the luminosity and extinction at fixed temperature, they are not reliable for determining a temperature (especially since they all lie on the

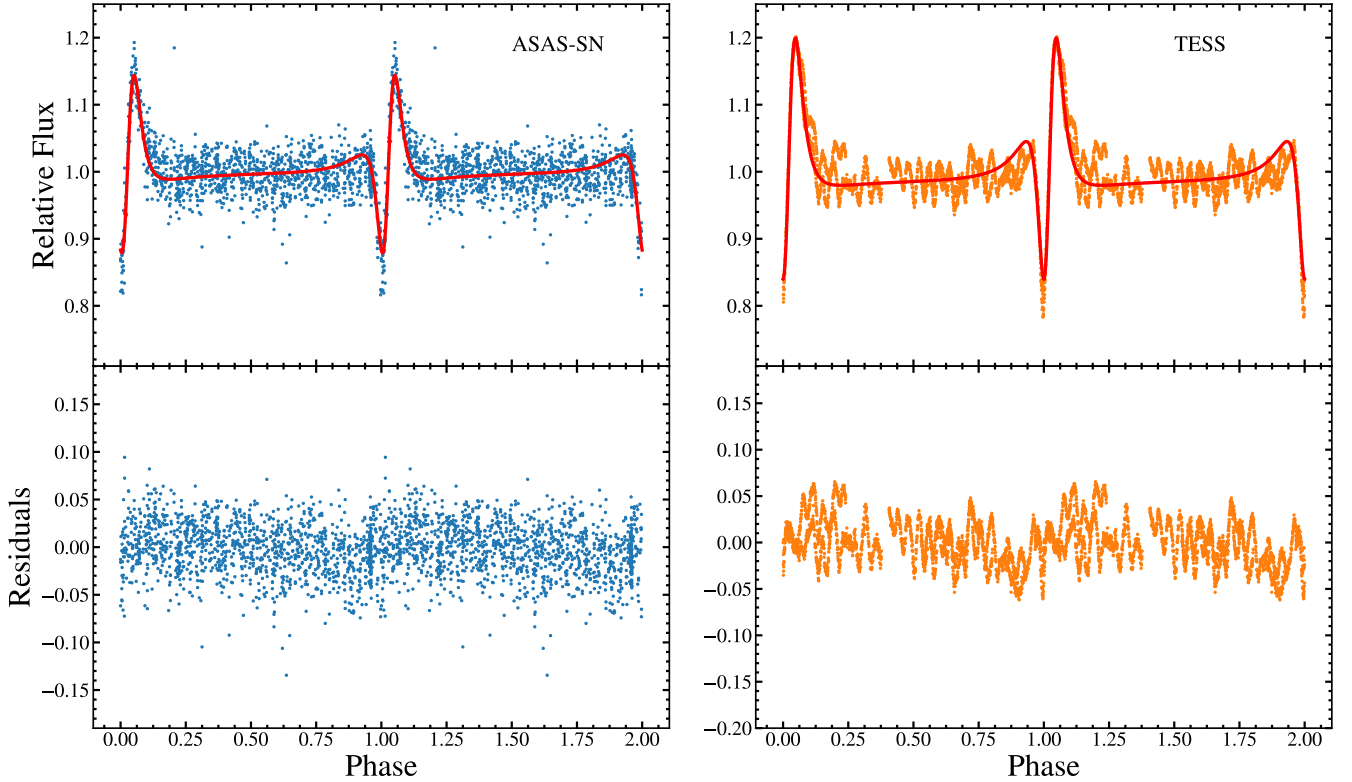


Figure 3. The phased ASAS-SN and TESS light curves (top) and residuals (bottom) for the source MACHO 80.7443.1718 after fitting with the Kumar et al. (1995) model for eccentric tidal distortions. Uncertainties in flux are not shown for clarity. The best-fit models are shown in red.

Table 2. Photometry used in the SED fits

Magnitude	σ	Filter	Reference
12.411	0.033	[3.6]	Meixner et al. (2006)
12.300	0.030	[4.5]	Meixner et al. (2006)
13.255	0.007	I	Cioni et al. (2000)
12.978	0.023	J	Cioni et al. (2000)
13.56	0.10	V	Massey (2002)
13.67	0.10	B	Massey (2002)
12.83	0.10	U	Massey (2002)
13.43	0.10	R	Massey (2002)
13.020	0.022	J	Cutri et al. (2003)
12.833	0.022	H	Cutri et al. (2003)
12.734	0.030	K_s	Cutri et al. (2003)
12.630	0.038	U	Zaritsky et al. (2004)
13.617	0.106	B	Zaritsky et al. (2004)
13.608	0.262	V	Zaritsky et al. (2004)
13.283	0.079	I	Zaritsky et al. (2004)

Rayleigh-Jeans side of the SED). The spectroscopic type, B0, indicates a temperature of $T_* \approx 25,000$ K, and for this temperature $\log(L_*/L_\odot) = 5.55 \pm 0.02$ with $E(B-V) \approx 0.47 \pm 0.02$ mag. Based on their photometry, Massey (2002) suggest a higher temperature of $T_* \approx 39,000$ K, which drives the luminosity and extinction up to $\log(L_*/L_\odot) = 6.09 \pm 0.02$ and $E(B-V) \approx 0.55 \pm 0.02$ mag. We view the spectroscopic temperature as being more reliable, but our general conclusions depend weakly on the adopted stellar temperature.

The results of the SED fits confirm that the source lies in the

LMC. The estimated Galactic extinction towards the source is only $E(B-V) \approx 0.06$ mag (Schlafly & Finkbeiner 2011), while the fits require $E(B-V) \approx 0.5$ mag and the LMC is the only likely source of the additional extinction. If we tried to make the star a 25,000 K main sequence star with $L \approx 10^{3.5} L_\odot$, it would lie at a distance of 5 kpc where such young, massive stars should not exist.

For the $T_* = 25,000$ K SED models, the stellar radius is $R_* \approx 32R_\odot$. The implied mass is trickier because it depends on the extent to which it is possible to have stripped mass from the star while maintaining a B0 spectral type. In the PARSEC (Tang et al. 2014) models, stars with $T_* \approx 25,000$ K and $L_* \approx 10^{5.55} L_\odot$ have $M_* \sim 30M_\odot$ and are starting to evolve across the Hertzsprung gap. The implied mass increases if we assume the higher temperature of Massey (2002).

If we combine the stellar radius, the orbital period, and the estimated eccentricity, we can see why the variability amplitudes are so high. The period and Kepler's third law imply that the orbital semi-major axis is

$$a = 93 \left(\frac{M_* + M_c}{10M_\odot} \right)^{1/2} R_\odot \quad (7)$$

where $M_* \approx 30M_\odot$ is the mass of the star and M_c is the mass of the unobserved companion. If we assume $e = 0.565$ from the fits in section §3 to the ellipsoidal distortions, then the pericentric radius $R_p = a(1-e)$ in terms of the stellar radius $R_* \approx 32R_\odot$ is

$$\frac{R_p}{R_*} \approx 1.26 \left(\frac{M_* + M_c}{10M_\odot} \right)^{1/2}, \quad (8)$$

so having $R_p = 2R_*$ implies $M_* + M_c \approx 25M_\odot$, and to reach

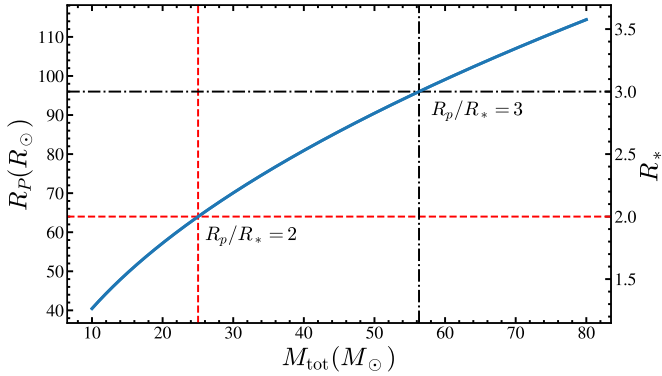


Figure 4. The total mass of the system against the periastron distance. The points at which $R_p/R_* = 2$ and $R_p/R_* = 3$ are shown as red and black dashed lines respectively.

$R_p = 3R_*$ implies $M_* + M_c \simeq 56M_\odot$ (Figure 4). Since the observed luminosity implies that the visible star is massive, it appears that the unobserved secondary must also be a massive object unless the pericentric approach distance is remarkably small.

There is no evidence of accretion (e.g., there seems to be no associated X-ray source in the ROSAT PSPC catalog of X-ray sources in the LMC (Haberl & Pietsch 1999) and we do not find any *Chandra*/XMM-Newton data), which probably requires that the pericenter lies outside the Roche limit. This essentially requires that the mass ratio $q = M_c/M_* < 1$, since placing the pericenter at the Roche limit for $q = 1$ implies $R_p/R_* \simeq 2.6$ and $M_* + M_c > 40M_\odot$. Assuming the companion is not a black hole, this is consistent with the absence of evidence for emission from the companion star in the SED fits. If we use the Morris (1985) estimate for the amplitude of the ellipsoidal variability using the pericentric distance for the orbital radius, it is difficult to get amplitudes above 0.1 – 0.2 mag, consistent with our attempts to model the system with PHOEBE 2.1, without the pericenter lying inside the Roche radius. However, this is an extrapolation of the Morris (1985) models for both the amplitude and the orbit, so we simply take this as further qualitative evidence that the pericentric radius is $R_p \simeq 2R_*$.

5 TIDALLY EXCITED OSCILLATIONS

With an approximate model for the tidal distortions, we can subtract the effect of the impulsive forcing and search for tidally excited oscillations (TEOs). TEOs occur at integer multiples of the orbital frequency, thus we carefully consider the orbital harmonics in the FFT spectrum. We calculated the Fast Fourier Transform (FFT) of the residuals using the *Period04* software package (Lenz & Breger 2005) and kept only harmonics with signal-to-noise ratios (SNRs) > 2 for further study. The frequencies were optimized to reduce the light curve residuals.

We also repeated this analysis for the TESS residuals. The combined TESS light curve shows significant variations outside of periastron with good SNR when compared to the ASAS-SN light curve. In order to reduce the impact of the tidal distortions on this calculation for both the ASAS-SN and TESS data, we only select the epochs with phases in the range [0.25, 0.85] (see Figure 1). Due to the time-sampling properties and the limited baseline of the TESS data, the FWHM of the peaks in the FFT power spectrum differ (Figure 4).

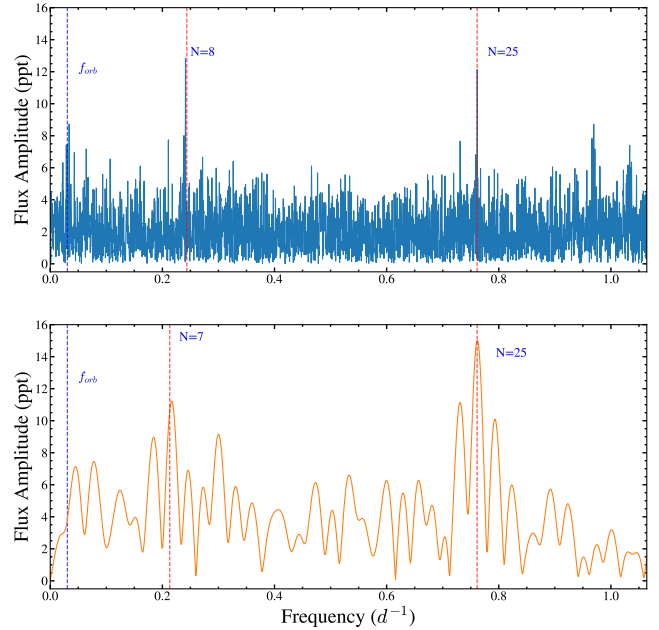


Figure 5. FFT spectrum of the residuals after subtracting the best-fit tidal distortion model from the ASAS-SN V-band data (top) and TESS data (bottom).

Figure 5 illustrates the FFT power spectrum for the residuals after fitting the best-fit tidal distortion model to the ASAS-SN and TESS data. The significant orbital harmonics are highlighted in red. In the FFT spectrum for the ASAS-SN residuals, we note significant peaks close to $f \sim 1 d^{-1}$. These are likely caused by aliasing and are absent in the TESS spectrum. The TEOs with SNR > 2 are summarized in Table 3. We calculated the uncertainty in the frequencies, amplitudes and phases, using the Monte Carlo simulation in *Period04*.

The orbital harmonic corresponding to the $N = 25$ mode ($P = 1.312$ d) was recovered from both the ASAS-SN and TESS data with SNR > 3 . Furthermore, we recover a TEO for the $N = 8$ mode in ASAS-SN data and a TEO corresponding to the $N = 7$ mode in TESS. The final multi-sector TESS light curve will provide a significantly better characterization of the TEOs.

6 CONCLUSIONS

We discovered that the variable star MACHO 80.7443.1718 is actually the highest amplitude heartbeat star discovered to date rather than an eclipsing binary. Using both the ASAS-SN and the TESS light curves, we find that MACHO 80.7443.1718 displays extreme flux variations for a variable of its kind, with maximal variations of $\sim 40\%$ at periastron and variations of $\sim 10\%$ due to tidally induced pulsations outside periastron. We fit an analytical model to the light curve to account for the variations caused by tidal distortions and estimated the orbital parameters for this system to be $\omega = -61.4^\circ$, $i = 44.8^\circ$ and $e = 0.566$. A more complete model of the system incorporating radial velocity information should improve our constraints of the orbital parameters. The star appears to have tidally induced pulsations at the $N = 7/8$, and 25 harmonics of the orbital period.

MACHO 80.7443.1718 is quite unlike any other heartbeat sys-

Table 3. Pulsation frequencies for MACHO 80.7443.1718, phased to periastron. The errors in frequency, amplitude and phase are calculated through a Monte Carlo analysis.

Data	Frequency ν (d^{-1})	Orbital Harmonic	ν/ν_{orb}	Amplitude (ppt)	Phase	SNR
ASAS-SN	0.24110 ± 0.01200	8	0.990	8.2 ± 4.2	0.457 ± 0.252	3.5
	0.76142 ± 0.00695	25	1.000	7.4 ± 4.5	0.120 ± 0.225	3.2
TESS	0.21638 ± 0.0004	7	1.015	11.1 ± 0.6	0.180 ± 0.008	2.7
	0.76189 ± 0.0006	25	1.000	14.9 ± 0.6	0.283 ± 0.006	4.7

tem discovered — it is both massive and extremely variable for its type. The identification of this source in ASAS-SN and its further characterization using data from the TESS satellite highlights the excellent synergy between these two projects. ASAS-SN is a long baseline survey and provides all-sky light curves that are well suited to study long term variability, whereas TESS light curves are more precise and sampled at a more rapid cadence even though they have a shorter baseline than ASAS-SN. The combination of data from these two surveys will advance the study of variability across the whole sky.

For a more complete characterization of this fascinating system, a radial-velocity follow-up campaign is necessary. These massive heartbeat stars should advance our understanding of the intricacies of stellar evolution and mergers in binary star systems. Furthermore, the tidally induced pulsations in these massive heartbeat systems also probe stellar structure and test theories of dynamical tides.

ACKNOWLEDGEMENTS

We thank the anonymous referee for their useful comments. We thank the Las Cumbres Observatory and its staff for its continuing support of the ASAS-SN project. We thank Jim Fuller for useful comments.

ASAS-SN is supported by the Gordon and Betty Moore Foundation through grant GBMF5490 to the Ohio State University and NSF grant AST-1515927. Development of ASAS-SN has been supported by NSF grant AST-0908816, the Mt. Cuba Astronomical Foundation, the Center for Cosmology and AstroParticle Physics at the Ohio State University, the Chinese Academy of Sciences South America Center for Astronomy (CASSACA), the Villum Foundation, and George Skestos. This work is supported in part by Scialog Scholar grant 24216 from the Research Corporation. CSK is supported by NSF grants AST-1515876, AST-1515927 and AST-181440. TAT acknowledges support from a Simons Foundation Fellowship and from an IBM Einstein Fellowship from the Institute for Advanced Study, Princeton.

This paper includes data collected by the TESS mission, which are publicly available from the Mikulski Archive for Space Telescopes (MAST). Funding for the TESS mission is provided by NASA's Science Mission directorate.

This work has made use of data from the European Space Agency (ESA) mission *Gaia* (<https://www.cosmos.esa.int/gaia>), processed by the *Gaia* Data Processing and Analysis Consortium (DPAC, <https://www.cosmos.esa.int/web/gaia/dpac/consortium>). This paper utilizes public domain data obtained by the MACHO Project, and has also made use of the VizieR catalogue access tool, CDS, Strasbourg, France. This re-

search was made possible through the use of the AAVSO Photometric All-Sky Survey (APASS), funded by the Robert Martin Ayers Sciences Fund.

REFERENCES

- Adams, S. M., & Kochanek, C. S. 2015, *MNRAS*, 452, 2195
Alard, C. 2000, *A&AS*, 144, 363
Alard, C., & Lupton, R. H. 1998, *ApJ*, 503, 325
Alcock, C., Allsman, R. A., Alves, D., et al. 1997, *ApJ*, 486, 697
Bhatti, W., Bouma, L. G., Wallace, J., et al. 2018, *astrobase*, v0.3.8, Zenodo, <http://doi.org/10.5281/zenodo.1185231>
Burkart, J., Quataert, E., Arras, P., et al. 2012, *MNRAS*, 421, 983.
Cardelli, J. A., Clayton, G. C., & Mathis, J. S. 1989, *ApJ*, 345, 245
Castelli, F., & Kurucz, R. L. 2004, *arXiv:astro-ph/0405087*
Cioni, M.-R. L., van der Marel, R. P., Loup, C., & Habing, H. J. 2000, *A&A*, 359, 601
Clarke, D. 2002, *A&A*, 386, 763
Cutri, R. M., Skrutskie, M. F., van Dyk, S., et al. 2003, *VizieR Online Data Catalog*, 2246,
Elitzur, M., & Ivezić, Ž. 2001, *MNRAS*, 327, 403
Fuller, J., & Lai, D. 2012, *MNRAS*, 420, 3126.
Fuller, J. 2017, *MNRAS*, 472, 1538.
Foreman-Mackey, D., Hogg, D. W., Lang, D., et al. 2013, *PASP*, 125, 306
Gaia Collaboration, Brown, A. G. A., Vallenari, A., et al. 2018, *arXiv:1804.09365*
Garmany, C. D., Massey, P., & Parker, J. W. 1994, *AJ*, 108, 1256.
Haberl, F., & Pietsch, W. 1999, *A&AS*, 139, 277
Hambleton, K., Fuller, J., Thompson, S., et al. 2018, *MNRAS*, 473, 5165.
Henden, A. A., Levine, S., Terrell, D., & Welch, D. L. 2015, *American Astronomical Society Meeting Abstracts #225*, 225, 336.16
Horvat, M., Conroy, K. E., Pablo, H., et al. 2018, *ApJS*, 237, 26
Ivezić, Z., & Elitzur, M. 1997, *MNRAS*, 287, 799
Jayasinghe, T., Kochanek, C. S., Stanek, K. Z., et al. 2018, *MNRAS*, 477, 3145
Jayasinghe, T., Stanek, K. Z., Kochanek, C. S., et al. 2019, *MNRAS*, 486, 1907
Jayasinghe T., et al., 2019, *MNRAS*, 485, 961
Kirk, B., Conroy, K., Prša, A., et al. 2016, *AJ*, 151, 68
Kochanek, C. S., Shappee, B. J., Stanek, K. Z., et al. 2017, *PASP*, 129, 104502
Kovács, G., Zucker, S., & Mazeh, T. 2002, *A&A*, 391, 369
Kumar, P., Ao, C. O., & Quataert, E. J. 1995, *ApJ*, 449, 294
Lafler, J., & Kinman, T. D. 1965, *ApJS*, 11, 216
Lenz, P., & Breger, M. 2005, *Communications in Asteroseismology*, 146, 53.
Lindgren, L., Hernández, J., Bombrun, A., et al. 2018, *A&A*, 616, A2.
Massey, P. 2002, *The Astrophysical Journal Supplement Series*, 141, 81.
Maceroni, C., Montalbán, J., Michel, E., et al. 2009, *A&A*, 508, 1375.
Meixner, M., Gordon, K. D., Indebetouw, R., et al. 2006, *AJ*, 132, 2268.

- Morris, S. L. 1985, *ApJ*, 295, 143
- Murray, C. D., & Correia, A. C. M. 2010, *Exoplanets*, 15.
- Nieva, M.-F., & Przybilla, N. 2014, *A&A*, 566, A7.
- Pablo, H., Richardson, N. D., Fuller, J., et al. 2017, *MNRAS*, 467, 2494.
- Pietrzyński, G., Graczyk, D., Gieren, W., et al. 2013, *Nature*, 495, 76
- Pedregosa, F., Varoquaux, G., Gramfort, A., et al. 2012, arXiv:1201.0490
- Prša, A., Conroy, K. E., Horvat, M., et al. 2016, *ApJS*, 227, 29
- Ricker, G. R., Winn, J. N., Vanderspek, R., et al. 2015, *Journal of Astronomical Telescopes, Instruments, and Systems*, 1, 014003
- Scargle, J. D. 1982, *ApJ*, 263, 835
- Schlafly, E. F., & Finkbeiner, D. P. 2011, *ApJ*, 737, 103
- Schwarzenberg-Czerny, A. 1996, *ApJ*, 460, L107
- Shappee, B. J., Prieto, J. L., Grupe, D., et al. 2014, *ApJ*, 788, 48
- Shporer, A., Fuller, J., Isaacson, H., et al. 2016, *ApJ*, 829, 34.
- Tang, J., Bressan, A., Rosenfield, P., et al. 2014, *MNRAS*, 445, 4287
- Thompson, S. E., Everett, M., Mullally, F., et al. 2012, *ApJ*, 753, 86.
- Watson, C. L., Henden, A. A., & Price, A. 2006, *Society for Astronomical Sciences Annual Symposium*, 25, 47
- Welsh, W. F., Orosz, J. A., Aerts, C., et al. 2011, *The Astrophysical Journal Supplement Series*, 197, 4.
- Zechmeister, M., & Kürster, M. 2009, *A&A*, 496, 577
- Zaritsky, D., Harris, J., Thompson, I. B., & Grebel, E. K. 2004, *AJ*, 128, 1606

This paper has been typeset from a $\text{\TeX}/\text{\LaTeX}$ file prepared by the author.